3

Strain in rocks

Strain can be retrieved from rocks through a range of different methods. Much attention has been paid to one-, two- and three-dimensional strain analyses in ductilely deformed rocks, particularly during the last half of the twentieth century, when a large portion of the structural geology community had their focus on ductile deformation. Strain data were collected or calculated in order to understand such things as thrusting in orogenic belts and the mechanisms involved during folding of rock layers. The focus of structural geology has changed and the field has broadened during the last couple of decades. Today strain analysis is at least as common in faulted areas and rift basins as in orogenic belts. While we will return to strain in the brittle regime in Chapter 21, we will here concentrate on classic aspects of how strain is measured and quantified in the ductile regime

The e-module for this chapter, *Strain*, provides further support on the following topics:

- Strain
- Breddin graph
- Wellman method
- R_f/ϕ method
- Fry method
- 3D strain

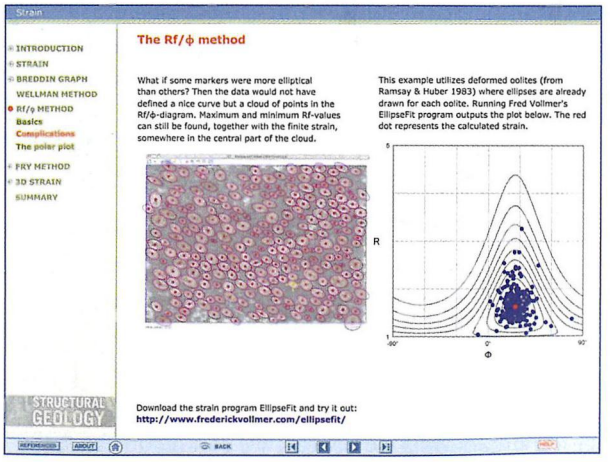

3.1 Why perform strain analysis?

It can be important to retrieve information about strain from deformed rocks. First of all, strain analysis gives us an opportunity to explore the state of strain in a rock and to map out strain variations in a sample, an outcrop or a region. Strain data are important in the mapping and understanding of shear zones in orogenic belts. Strain measurements can also be used to estimate the amount of offset across a shear zone. As will be discussed in Chapter 16, it is possible to extract important information from shear zones if strain is known.

In many cases it is useful to know if the strain is planar or three-dimensional. If planar, an important criterion for section balancing is fulfilled, be it across orogenic zones or extensional basins. The shape of the strain ellipsoid may also contain information about how the deformation occurred. Oblate (pancake-shaped) strain in an orogenic setting may, for example, indicate flattening strain related to gravity-driven collapse. However, flattening is also a characteristic feature of a deformation type known as transpression (Chapter 19), so be aware that a given strain can be formed in more than one way.

The orientation of the strain ellipsoid is also important, particularly in relation to rock structures. In a shear zone setting, it may tell us if the deformation was simple shear or not (Chapter 16). Strain in folded layers helps us to understand fold-forming mechanism(s) (Chapter 12). Studies of deformed reduction spots in slates give good estimates on how much shortening has occurred across the foliation in such rocks (Chapter 13), and strain markers in sedimentary rocks can sometimes allow for reconstruction of original sedimentary thickness. Strain will follow us through most of this book.

3.2 Strain in one dimension

One-dimensional strain analyses are concerned with changes in length and therefore the simplest form of strain analysis we have. If we can reconstruct the original length of an object or linear structure we can also calculate the amount of stretching or shortening in that direction. Objects revealing the state of strain in a deformed rock are known as **strain markers**. Examples of strain markers indicating change in length are boudinaged dikes or layers, and minerals or linear fossils such as belemnites or graptolites that have been elongated, such as the stretched Swiss belemnites shown in Figure 3.1. Other examples could be a layer shortened by folding, or a faulted reference horizon on a geologic or seismic profile, as will be discussed in Chapter 21. The horizon may be stretched by normal faults (Figure 2.7) or shortened by reverse faults, and the overall strain is referred to as **fault strain** or **brittle strain**. One-dimensional strain is revealed when the horizon, fossil, mineral or dike is restored to its pre-deformational state.

Figure 3.1 Two elongated belemnites in Jurassic limestone in the Swiss Alps. The different ways that the two belemnites have been stretched give us some two-dimensional information about the strain field: the upper belemnite has experienced sinistral shear strain while the lower one has not and must be close to the maximum stretching direction.

3.3 Strain in two dimensions

In **two-dimensional strain analyses** we look for sections that have objects of known initial shape or contain linear markers with a variety of orientations (Figure 3.1). Strained reduction spots (Box 3.1) are frequently used as an example, because undeformed reduction spots tend to have spherical shapes in undeformed sedimentary rocks. There are also many other types of objects that can be used, such as sections through conglomerates, breccias, corals, oolites, vesicles, pillow lavas, columnar basalt, and augen gneiss (Figure 3.2). Two-dimensional strain can also be calculated from one-dimensional data that represent different directions in the same section. A typical example would be dikes with different orientations that show different amounts of extension.

Strain extracted from sections is the most common type of strain data, and sectional data can be combined to estimate the three-dimensional strain ellipsoid.

Changes in angles

Strain can be found if we know the original angle between sets of lines. The original angular relations between structures such as dikes, foliations and bedding are sometimes found in both undeformed and deformed states, i.e. outside and inside a deformation zone. We can then see how

BOX 3.1 REDUCTION SPOTS AND STRAIN

Reduction spots in reddish sedimentary rocks form around ore minerals or organic particles as they oxidize and reduce the surrounding host rock. During this process reddish hematite pigment is reduced and the rock becomes pale greenish or yellowish. When reduction spots form in homogeneous sedimentary rocks, the reduction extends the same distance from the nucleus in all directions, and the result is a spherical geometry. If the rock gets deformed and the reduction spots are preserved, they would represent perfect strain markers because there is no competence contrast between the spots and the host rock. Hence, where reduction spots are found in very low-grade slates, such as the classical Welsh slates or similar slates in Vermont, it is generally assumed that these are reduction spots that formed prior to deformation, hence reflecting the strain involved during the slate-forming deformation (generally flattening, with more than 60% shortening across the cleavage).

An alternative interpretation is that the reduction happened after deformation by infiltration by reducing fluid such as CO_2, and that the reason for the elliptical shapes is the anisotropy represented by the cleavage, where diffusion is faster parallel than perpendicular to the cleavage. Magnetic studies indicate that this may be the case in some slates, suggesting that we have to be careful about how we interpret elliptical markers in deformed slates.

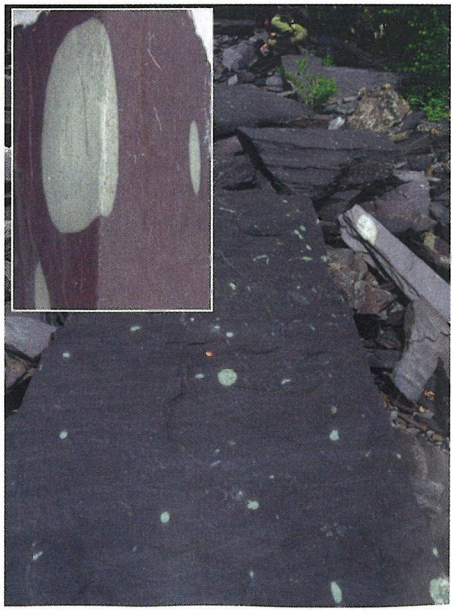

Reduction spots in slate from the Taconic slate belt of Vermont (Cedar Point quarry) and from Wales (inset).

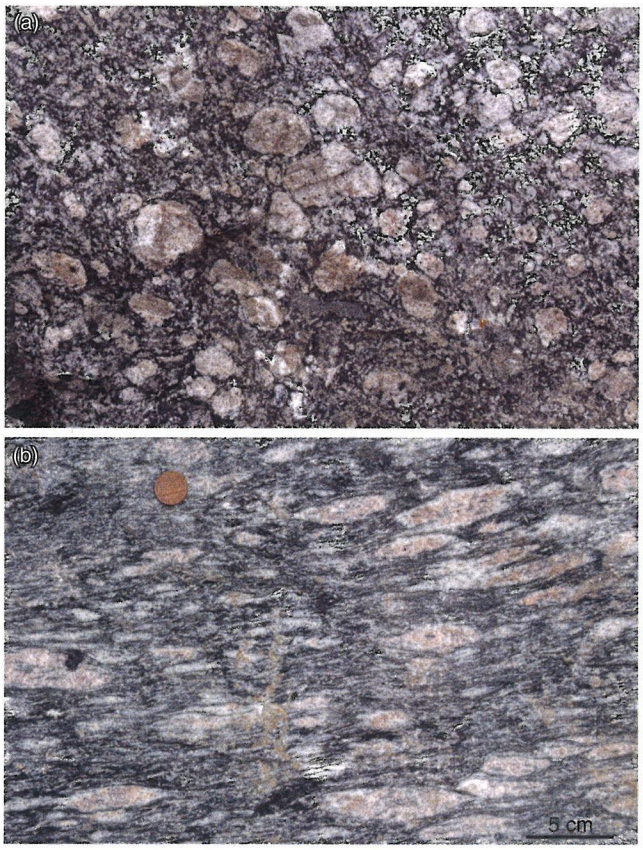

Figure 3.2 Two sections through granitic augen gneiss. In (a) the potassium feldspar porphyroblasts are fairly equidimensional with no preferred orientation in a non-foliated matrix, while in (b) they are elongated and parallel to the foliation in the matrix. Both sections are from the same deformed rock, but (a) experienced area reduction, i.e. only shrinkage and no change in shape. Western Gneiss Region, Norwegian Caledonides.

the strain has affected the angular relationships and use this information to estimate strain. In other cases orthogonal lines of symmetry found in undeformed fossils such as trilobites, brachiopods and worm burrows (angle with layering) can be used to determine the angular shear in some deformed sedimentary rocks (Figure 3.3). In general, all we need to know is the change in angle between sets of lines and that there is no strain partitioning due to contrasting mechanical properties of the objects with respect to the enclosing rock.

If the angle was 90° in the undeformed state, the change in angle is the local angular shear ψ (Section 2.8). If, as we recall from Chapter 2, the two originally orthogonal lines remain orthogonal after the deformation, then they must represent the principal strains and thus the orientation of the strain ellipsoid. Observations of variously oriented line sets thus give information about the strain ellipse or ellipsoid. All we need is a useful method. Two of the most common methods used to find strain from initially

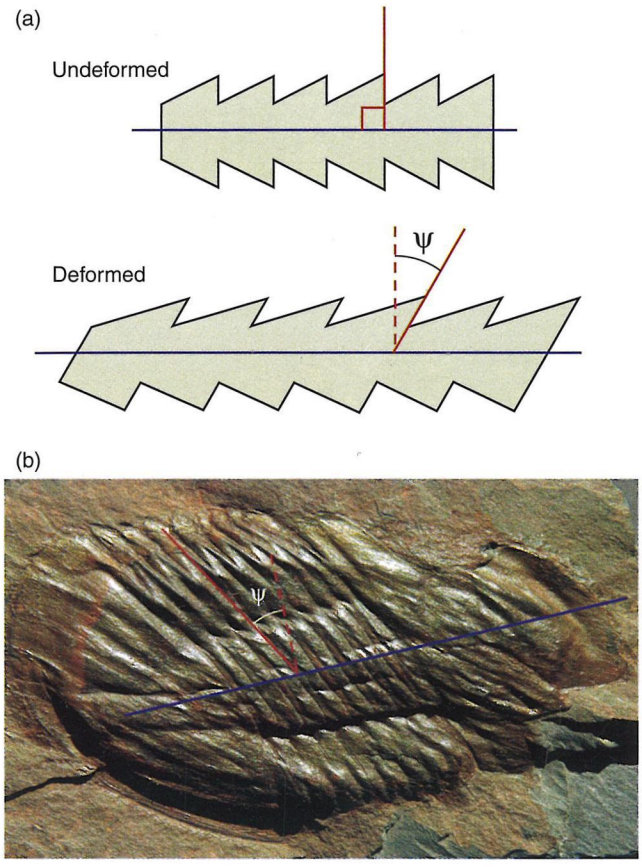

Figure 3.3 Change in angles (angular shear strain, Ψ) as determined from (a) deformed graptolites and (b) deformed trilobite (see Figure 2.9). The angular shear strain can be determined based on the knowledge about initial symmetry from undeformed samples of the species. See Goldstein (1998) for more information about deformed graptolites. Trilobite photo by Marli Miller (Asaphellus murchisoni from Wales).

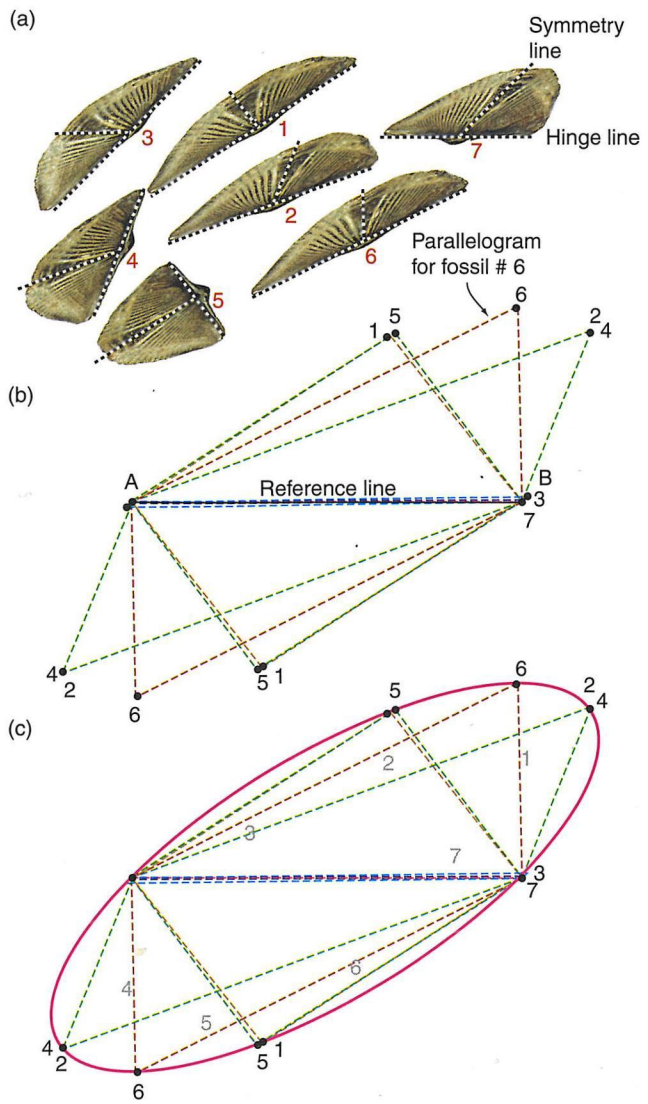

Figure 3.4 Wellman's method involves construction of the strain ellipse by drawing parallelograms based on the orientation of originally orthogonal pairs of lines. The deformation was produced on a computer and is a homogeneous simple shear of $\gamma = 1$. However, the strain ellipse itself tells us nothing about the degree of coaxiality: the same result could have been attained by pure shear.

orthogonal lines are known as the Wellman and Breddin methods, and are presented in the following sections.

The Wellman method

This method dates back to 1962 and is a geometric construction for finding strain in two dimensions (in a section). It is typically demonstrated on fossils with orthogonal lines of symmetry in the undeformed state. In Figure 3.4a we use the hinge and symmetry lines of brachiopods. A line of reference must be drawn (with arbitrary orientation) and pairs of lines that were orthogonal in the unstrained state are identified. The reference line must have two defined endpoints, named A and B in Figure 3.4b. A pair of lines is then drawn parallel to both the hinge line and symmetry line for each fossil, so that they intersect at the endpoints of the reference line. The other points of intersection are marked (numbered 1–6 in Figure 3.4b, c). If the rock is unstrained, the lines will define rectangles. If there is a strain involved, they will define parallelograms. To find the strain ellipse, simply fit an ellipse to the numbered corners of the parallelograms (Figure 3.4c). If no ellipse can be fitted to the corner points of the rectangles the strain is heterogeneous or, alternatively, the measurement or assumption of initial orthogonality is false. The challenge with this method is, of course, to find enough fossils or other features with initially orthogonal lines – typically 6–10 are needed.

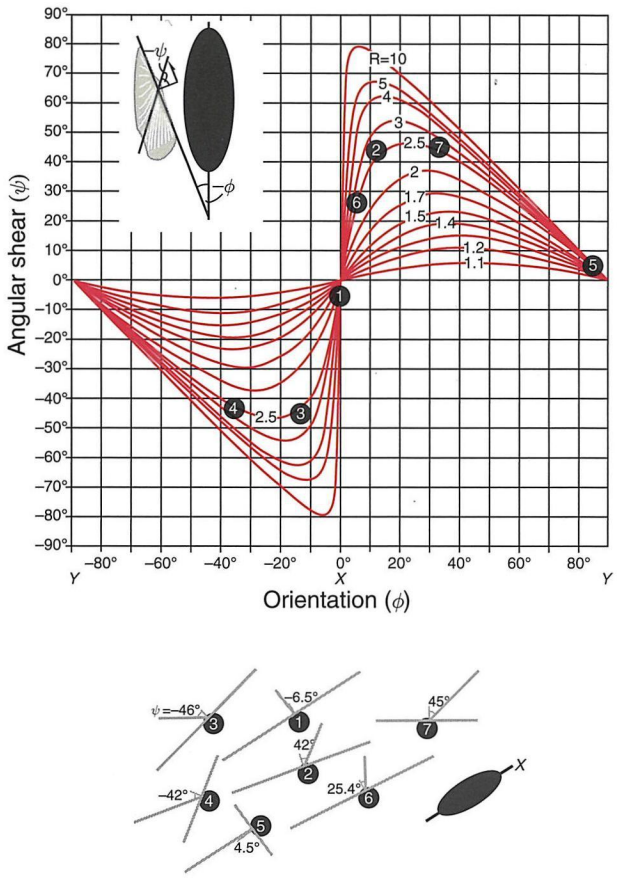

Figure 3.5 The data from Figure 3.5 plotted in a Breddin graph. The data points are close to the curve for $R = 2.5$.

The Breddin graph

We have already stated that the angular shear depends on the orientation of the principal strains: the closer the deformed orthogonal lines are to the principal strains, the lower the angular shear. This fact is utilized in a method first published by Hans Breddin in 1956 in German (with some errors). It is based on the graph shown in Figure 3.5, where the angular shear changes with orientation and strain magnitude R. Input are the angular shears and the orientations of the sheared line pairs with respect to the principal strains. These data are plotted in the so-called Breddin graph and the R-value (ellipticity of the strain ellipse) is found by inspection (Figure 3.5). This method may work even for only one or two observations.

In many cases the orientation of the principal axes is unknown. In such cases the data are plotted with respect to an arbitrarily drawn reference line. The data are then moved horizontally on the graph until they fit one of the curves, and the orientations of the strain axes are then found at the intersections with the horizontal axis (Figure 3.5). In this case a larger number of data are needed for good results.

Elliptical objects and the R_f/ϕ-method

Objects with initial circular (in sections) or spherical (in three dimensions) geometry are relatively uncommon, but do occur. Reduction spots and ooliths perhaps form the most perfect spherical shapes in sedimentary rocks. When deformed homogeneously, they are transformed into ellipses and ellipsoids that reflect the local finite strain. Conglomerates are perhaps more common and contain clasts that reflect the finite strain. In contrast to oolites and reduction spots, few pebbles or cobbles in a conglomerate are spherical in the undeformed state. This will of course influence their shape in the deformed state and causes a challenge in strain analyses. However, the clasts tend to have their long axes in a spectrum of orientations in the undeformed state, in which case methods such as the R_f/ϕ-method may be able to take the initial shape factor into account.

The R_f/ϕ-method was first introduced by John Ramsay in his 1967 textbook and was later improved. The method is illustrated in Figure 3.6. The markers are assumed to have approximately elliptical shapes in the deformed (and undeformed) state, and they must show a significant variation in orientations for the method to work.

The R_f/ϕ method handles initially non-spherical markers, but the method requires a significant variation in the orientations of their long axes.

The ellipticity (X/Y) in the undeformed (initial) state is called R_i. In our example (Figure 3.6) $R_i = 2$. After a strain R_s the markers exhibit new shapes. The new shapes are different and depend on the initial orientation of the elliptical markers. The new (final) ellipticity for each deformation marker is called R_f and the spectrum of R_f-values is plotted against their orientations, or more specifically against the angle ϕ' between the long axis of the ellipse and a reference line (horizontal in Figure 3.6). In our example we have applied two increments of pure shear to a series of ellipses with different orientations. All the ellipses have the same initial shape $R_i = 2$, and they plot along a vertical line in the upper right diagram in Figure 3.6. Ellipse 1 is oriented with its long axis along the minimum principal strain axis, and it is converted into an ellipse that shows less strain (lower R_f-value) than the true strain ellipse (R_s). Ellipse 7, on the other hand, is oriented with its long axis parallel to the long axis of the strain ellipse, and the two ellipticities are added. This leads to an ellipticity that is higher than R_s. When $R_s = 3$, the true strain R_s is located somewhere between the shape represented

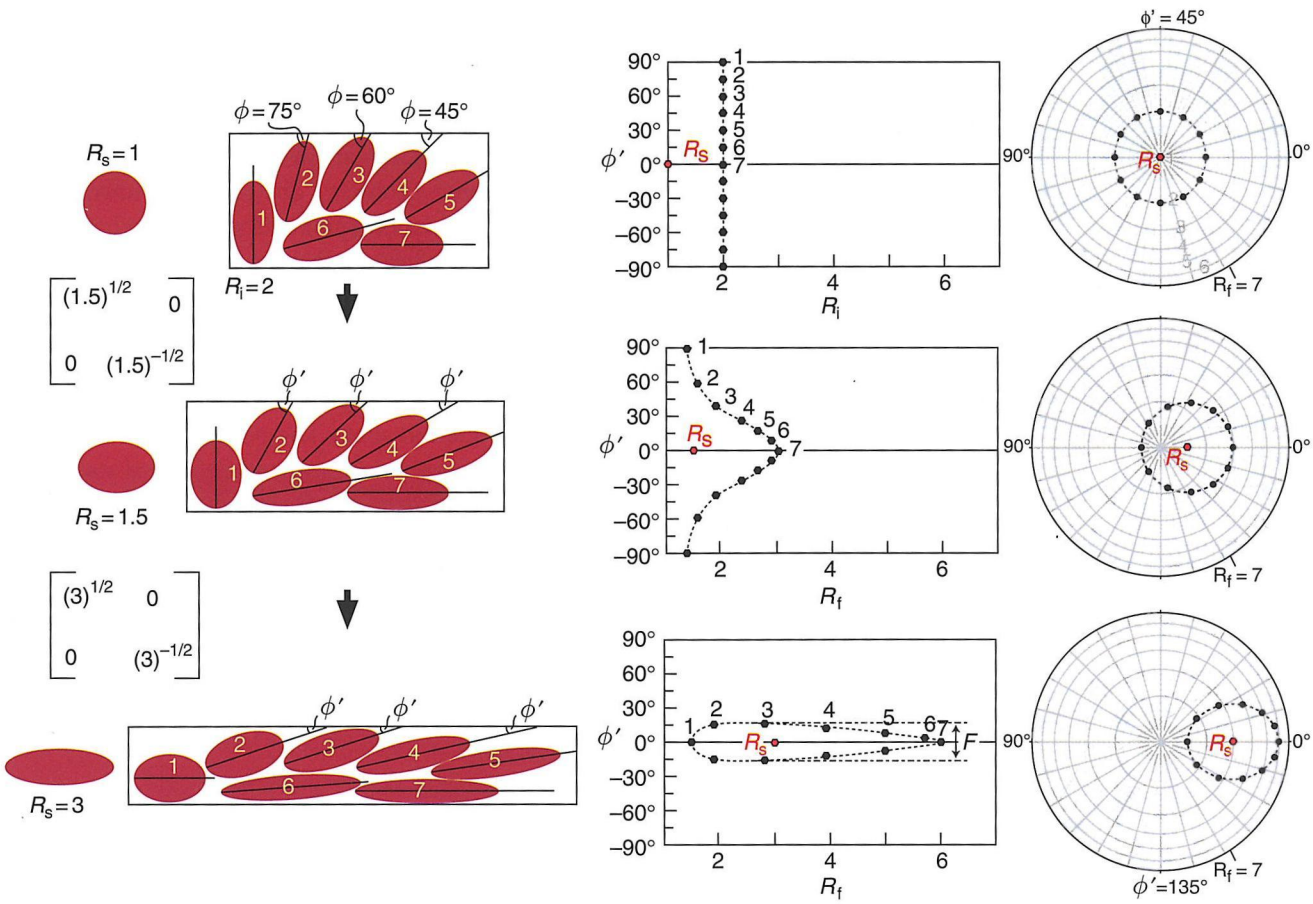

Figure 3.6 The R_f/ϕ method illustrated. The ellipses have the same ellipticity (R_i) before the deformation starts. The R_f–ϕ diagram to the right indicates that $R_i = 2$. A pure shear is then added with $R_s = 1.5$ followed by a pure shear strain of $R_s = 3$. The deformation matrices for these two deformations are shown. Note the change in the distribution of points in the diagrams to the right. R_s in the diagrams is the actual strain that is added. Right: The data presented in polar Elliot graphs. The software "EllipseFit" by Frederick W. Vollmer was used. Left part based on Ramsay and Huber (1983).

by ellipses 1 and 7, as seen in Figure 3.6 (lower right diagram).

For $R_s = 1.5$ we still have ellipses with the full spectrum of orientations (−90° to 90°; see middle diagram in Figure 3.6), while for $R_s = 3$ there is a much more limited spectrum of orientations (lower graph in Figure 3.6). The scatter in orientation is called the fluctuation F. An important change happens when ellipse 1, which has its long axis along the Z-axis of the strain ellipsoid, passes the shape of a circle ($R_s = R_i$,) and starts to develop an ellipse whose long axis is parallel to X. This happens when $R_s = 2$, and for larger strains the data points define a circular shape. Inside this shape is the strain R^s that we are interested in. But where exactly is R_s? A simple average of the maximum and minimum R_f-values would depend on the original distribution of orientations. Even if the initial distribution is random, the average R-value would be too high, as high values tend to be overrepresented (Figure 3.6, lower graph).

To find R_s we have to treat the cases where $R_s > R_i$ and $R_s < R_i$ separately. In the latter case, which is represented by the middle graph in Figure 3.6, we have the following expressions for the maximum and minimum value for R_f:

$$R_{fmax} = R_s R_i$$

$$R_{fmin} = R_i / R_s$$

Solving for R_i and R_s gives

$$R_s = (R_{fmax}/R_{fmin})^{1/2}$$

$$R_i = (R_{fmax} R_{fmin})^{1/2}$$

which represent expressions for both the strain related to the deformation and the initial ellipticity.

For higher-strain cases, where $R_s < R_i$, we obtain

$$R_{fmax} = R_s R_i$$

$$R_{fmin} = R_s / R_i$$

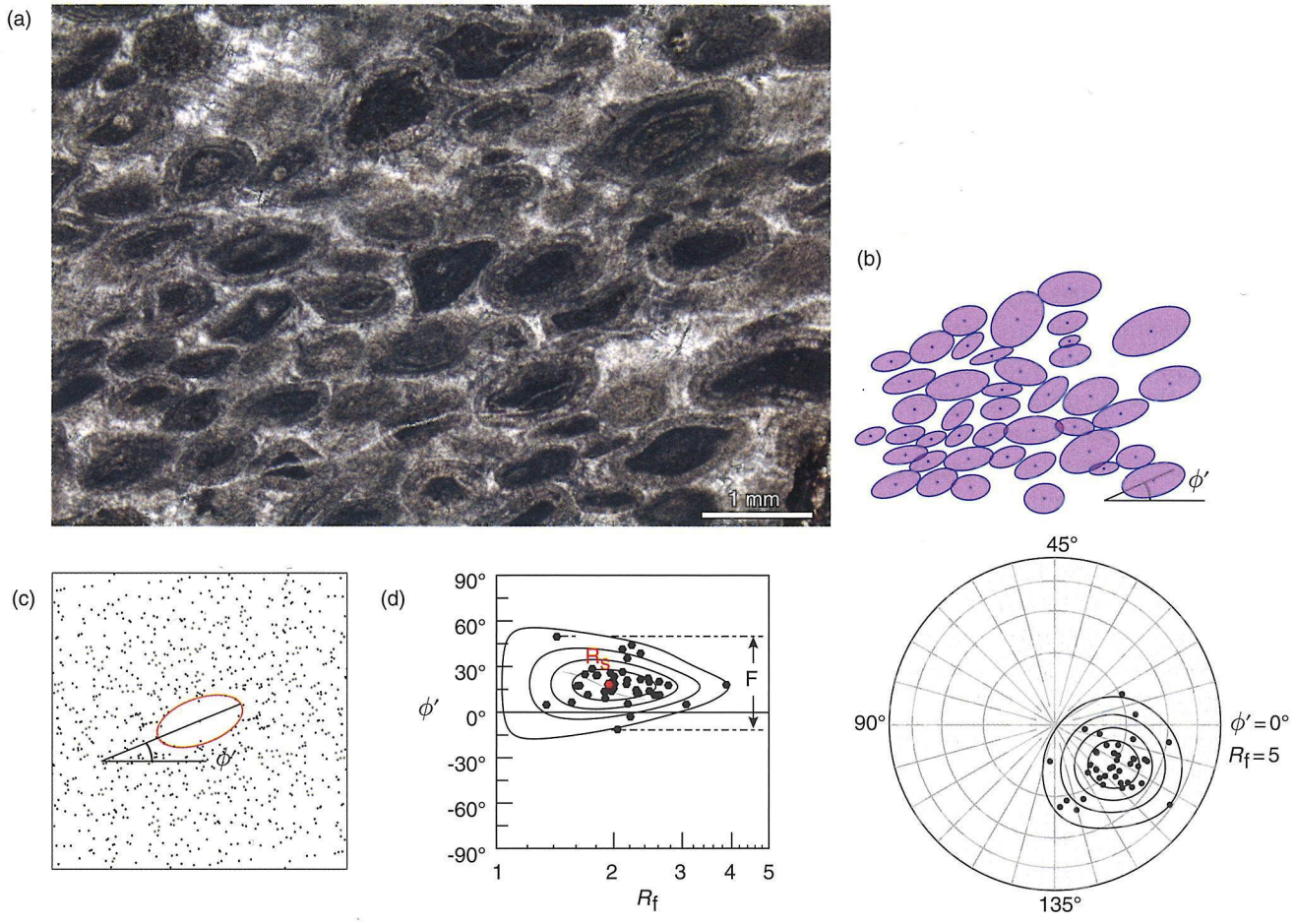

Figure 3.7 Naturally deformed oolites from Sardinia, analyzed by means of the software "EllipseFit" by Frederick W. Vollmer. Ellipses were drawn for a selection of ooids (b), and an R_f/ϕ diagram (c), Fry plot (d) and polar Elliott plot (e) were generated. Thin section photo by Alessandro Da Mommio.

Solving for R_s gives

$$R_s = (R_{fmax}/R_{fmin})^{1/2}$$

$$R_i = (R_{fmax}/R_{fmin})^{1/2}$$

In both cases the orientation of the long (X) axis of the strain ellipse is given by the location of the maximum R_f-values. Strain could also be found by fitting the data to pre-calculated curves for various values for R_i and R_s. In practice, such operations are most efficiently done by means of computer programs. An example of real data (oolites in thin section) is shown in Figure 3.7a–c. The strain (R_s-value) is found to be ~2 and the orientation is defined relative to the frame of the picture. To utilize this orientation, our thin section would need to be oriented.

As an alternative way of plotting R_f/ϕ data, we could use the polar Elliott graph, suggested by David Elliott in 1970, which plots R_f radially (from $R_f = 1$ in the center to a specified value along the primitive circle) versus 2 times ϕ. The polar Elliott graph greatly reduces the distortion produced by the regular R_f/ϕ plot, which is particularly noticeable at low strains.

The example shown in Figure 3.6 and discussed above is idealized in the sense that all the undeformed elliptical markers have identical ellipticity. What if this were not the case, i.e. some markers were more elliptical than others? Then the data would not have defined a nice curve but a cloud of points in the R_f/ϕ-diagram. Maximum and minimum R_f-values could still be found and strain could be calculated using the equations above. The only change in the equation is that R_i now represents the maximum ellipticity present in the undeformed state.

Another complication that may arise is that the initial markers may have had a restricted range of orientations. Ideally, the R_f/ϕ-method requires the elliptical objects to be more or less randomly oriented prior to deformation. Conglomerates, to which this method is commonly applied, tend to have clasts with a preferred orientation. This may result in an R_f–ϕ plot in which only a part of the curve or cloud is represented. In this case the maximum

and minimum R_f-values may not be representative, and the formulas above may not give the correct answer and must be replaced by a computer-based iterative retro-deformation method where X is input. However, many conglomerates have a few clasts with initially anomalous orientations that allow the use of R_f/ϕ analysis.

Center-to-center method

This method, here demonstrated in Figure 3.8, is based on the assumption that circular objects have a more or less statistically uniform distribution in our section(s). This means that the distances between neighboring particle centers were fairly constant before deformation. The particles could represent sand grains in well-sorted sandstone, pebbles, ooids, mud crack centers, pillow lava or pahoe-hoe lava centers, pluton centers or other objects that are of similar size and where the centers are easily definable. If you are uncertain about how closely your section complies with this criterion, try anyway. If the method yields a reasonably well-defined ellipse, then the method works.

The method itself is simple and is illustrated in Figure 3.8. Measure the distance and direction from the center of an ellipse to those of its neighbors. Repeat this for all ellipses and graph the distance d' between the centers and the angles α' between the center tie lines and a reference line. A straight line occurs if the section is unstrained, while a deformed section yields a curve with maximum (d'_{max}) and minimum values (d'_{min}). The ellipticity of the strain ellipse is then given by the ratio: $R_s = (d'_{max})/(d'_{min})$.

The Fry method

A quicker and visually more attractive method for finding two-dimensional strain was published by Norman Fry in 1979. This method, illustrated in Figure 3.9, is based on the center-to-center method and is most easily dealt with using one of several available computer programs. It can be done manually by placing a tracing overlay with a coordinate origin and pair of reference axes on top of a sketch or picture of the section. The origin is placed on a particle center and the centers of all other particles (not just the neighbors) are marked on the tracing paper. The tracing paper is then moved, without rotating the paper with respect to the section, so that the origin covers a second particle center, and the centers of all other particles are again marked on the tracing paper. This procedure is repeated until the area of interest has been covered. For objects with a more or less uniform distribution the result will be a visual representation of the strain ellipse. The ellipse is the void area in the middle, defined by the point cloud around it (Figure 3.9c). An example is shown in Figure 3.7d for deformed oolites.

The Fry method, as well as the other methods presented in this section, outputs two-dimensional strain.

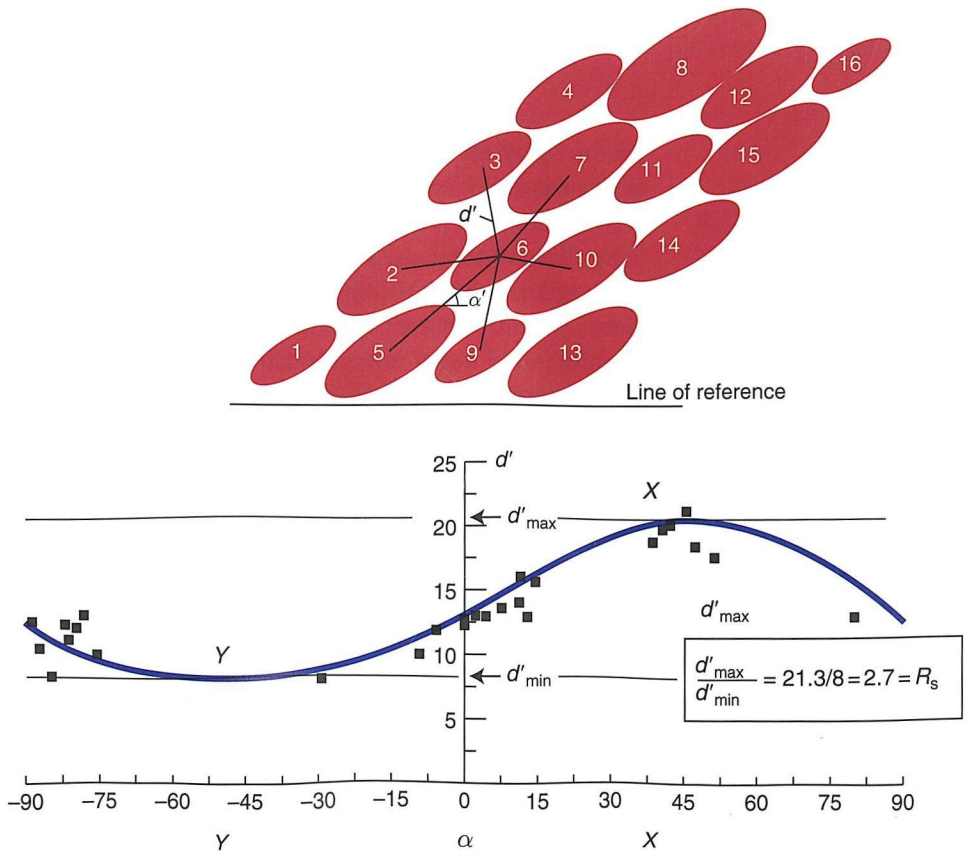

Figure 3.8 The center-to-center method. Straight lines are drawn between neighboring object centers. The length of each line (d') and the angle (α') that they make with a reference line are plotted in the diagram. The data define a curve that has a maximum at X and a minimum at the Y-value of the strain ellipse, and where $R_s = X/Y$.

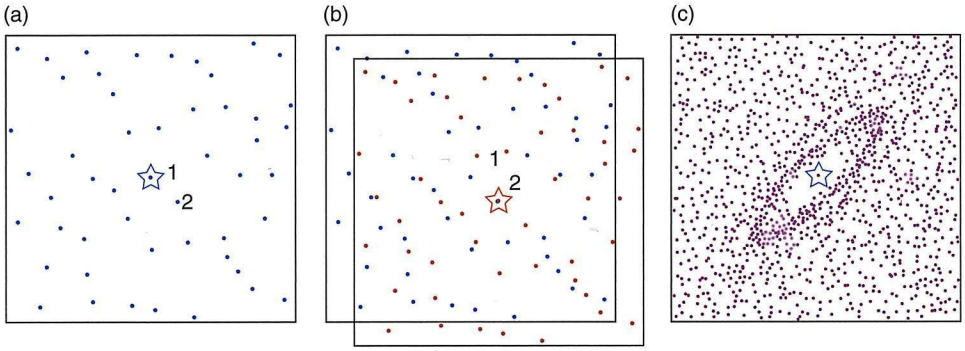

Figure 3.9 The Fry method performed manually. (a) The centerpoints for the deformed objects are transferred to a transparent overlay. A central point (1 on the figure) is defined. (b) The transparent paper is then moved to another of the points (point 2) and the centerpoints are again transferred onto the paper (the overlay must not be rotated). The procedure is repeated for all of the points, and the result (c) is an image of the strain ellipsoid (shape and orientation). Based on Ramsay and Huber (1983).

Three-dimensional strain is found by combining strain estimates from two or more sections through the deformed rock volume. If sections can be found that each contain two of the principal strain axes, then two sections are sufficient. In other cases three or more sections are needed, and the three-dimensional strain must be calculated by use of a computer.

3.4 Strain in three dimensions

A complete strain analysis is **three-dimensional**. Three-dimensional strain data are presented in the Flinn diagram or similar diagrams that describe the shape of the strain ellipsoid, also known as the **strain geometry**. In addition, the orientation of the principal strains can be presented by means of spherical projections. Direct field observations of three-dimensional strain are rare. In almost all cases, analysis is based on two-dimensional strain observations from two or more sections at the same locality (Figure 3.10). A well-known example of three-dimensional strain analysis from deformed conglomerates is presented in Box 3.1.

In order to quantify ductile strain, be it in two or three dimensions, the following conditions need to be met:

The strain must be homogeneous at the scale of observation, the mechanical properties of the objects must have been similar to those of their host rock during the deformation, and we must have a reasonably good knowledge about the original shape of strain markers.

The first point is obvious. If the strain is heterogeneous we have to look at another scale, either a larger one where the heterogeneities vanish, or subareas where strain can be considered to be approximately homogeneous. The latter was done in the example in Box 3.2, where a strain pattern

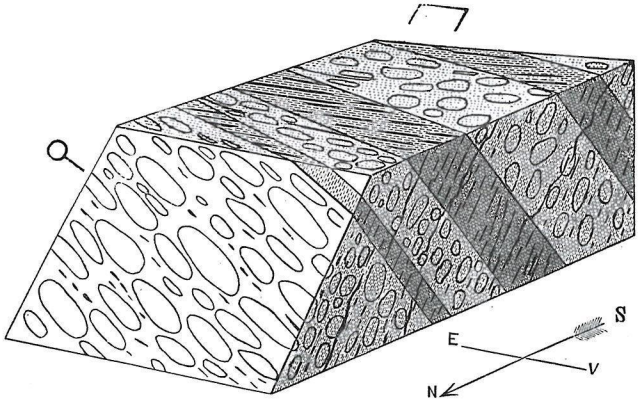

Figure 3.10 Three-dimensional strain expressed as ellipses on different sections through a conglomerate. The foliation *XY*-plane) and the lineation (*X*-axis) are annotated. This illustration was published in 1888, but what are now routine strain methods were not developed until the 1960s.

was mapped out that could be related to a larger structure. This example shows how mapping of the state of strain can help us to understand the formation of larger-scale structures, in this case the history of folding.

The second point is an important one. For ductile rocks it means that the object and its surroundings must have had the same competence or viscosity (see Chapter 5). Otherwise the strain recorded by the object would be different from that of its surroundings. This effect is one of several types of **strain partitioning**, where the overall strain is distributed unevenly in terms of intensity and/or geometry in a rock volume. As an example, we mark a perfect circle on a piece of clay before flattening it between two walls. The circle transforms passively into an ellipse that reveals the two-dimensional strain if the deformation is homogeneous. If we embed a colored sphere of the same clay, then it would again deform along with the

BOX 3.2 DEFORMED QUARTZITE CONGLOMERATES

Quartz or quartzite conglomerates with a quartzite matrix are commonly used for strain analyses. The more similar the mineralogy and grain size of the matrix and the pebbles, the less deformation partitioning and the better the strain estimates. A classic study of deformed quartzite conglomerates is Jake Hossack's study of the Norwegian Bygdin conglomerate, published in 1968. Hossack was fortunate – he found natural sections along the principal planes of the strain ellipsoid at each locality. Putting the sectional data together gave the three-dimensional state of strain (strain ellipsoid) for each locality. Hossack found that strain geometry and intensity varies within his field area. He related the strain pattern to static flattening under the weight of the overlying Caledonian Jotun Nappe. Although details of his interpretation may be challenged, his work demonstrates how conglomerates can reveal a complicated strain pattern that otherwise would have been impossible to map. Hossack noted the following sources of error:

- Inaccuracy connected with data collection (sections not being perfectly parallel to the principal planes of strain and measuring errors).
- Variations in pebble composition.
- The pre-deformational shape and orientation of the pebbles.
- Viscosity contrasts between clasts and matrix.
- Volume changes related to the deformation (pressure solution).
- The possibility of multiple deformation events.

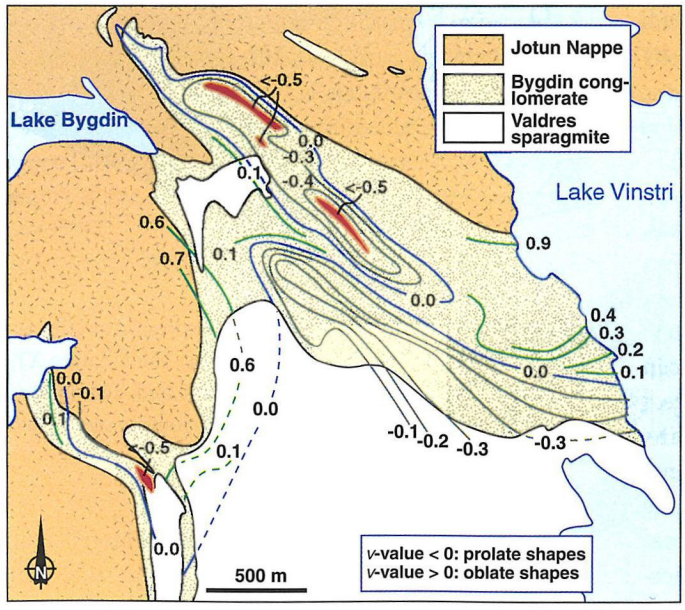

Hossack's strain map from the Bygdin area, Norway.

The Bygdin conglomerate.

rest of the clay, revealing the three-dimensional strain involved. However, if we put a stiff marble in the clay the result is quite different. The marble remains unstrained while the clay around it becomes more intensely and heterogeneously strained than in the previous case. In fact, it causes a more **heterogeneous strain** pattern to appear. Strain markers with the same mechanical properties as the surroundings are called **passive markers** because they deform passively along with their surroundings. Those that have anomalous mechanical properties respond

BOX 3.3 STRAIN AROUND A FOLD

Deformed conglomerates are an important source of strain data in deformed rocks because conglomerates are relatively common and contain large numbers of objects (clasts). An example is shown where strain was evaluated at several stations around a folded conglomerate layer, deformed under greenschist facies conditions. It was found that the long limbs were totally dominated by flattening strain (oblate strain geometry) while there was a change toward constrictional strain in the hinge and short limb area. This information would have been difficult to achieve without mesoscopic strain markers, because the rock is recrystallized so that the original sand grain boundaries are obliterated.

The strain distribution then had to be explained, and was found to fit a model where an already flattened conglomerate layer is rotated into the field of shortening during shearing. A dextral shear rotates the foliation and the oblate clasts into the shortening field, which makes the *Y*-axis shrink. This takes the strain ellipsoid across the plane strain diagonal of the Flinn diagram and into the constrictional field ($k > 1$). At this point we are on the inverted limb or at the lower fold hinge. The process continues, and the strain ellipse again becomes flattened. This model explains strain data by means of a particular deformation history, defining a certain strain path, which in this case is flattening to constriction and then back to flattening strain again.

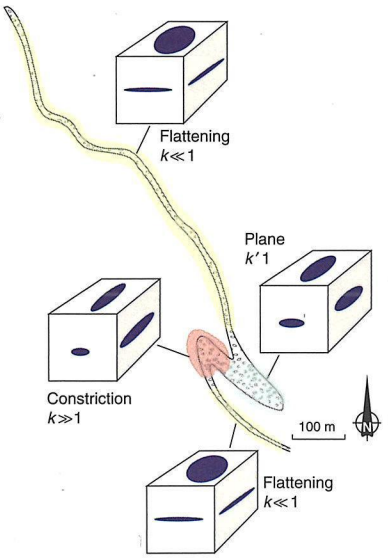

Map of the conglomerate layer. Note the thickened short fold limb.

The conglomerate in a constrictional state of strain.

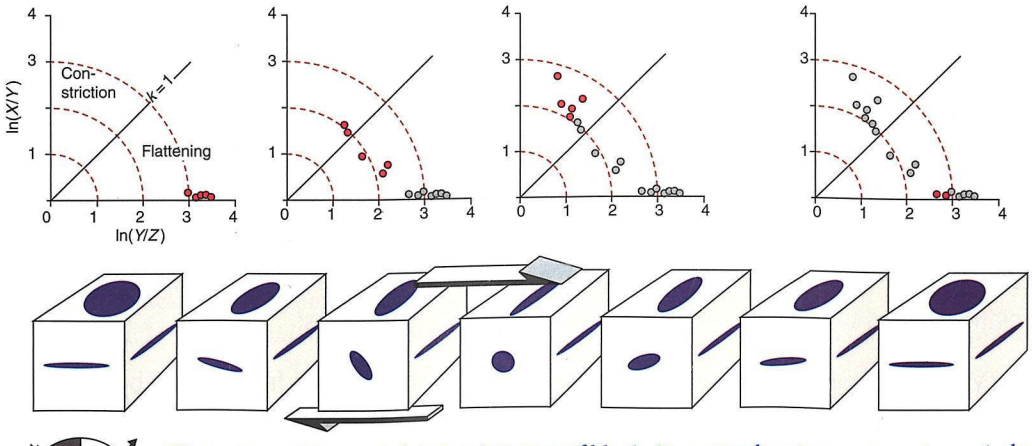

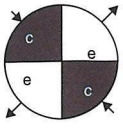

Illustration of the strain history in terms of block diagrams showing sections through the strain ellipsoid and strain data plotted in Flinn diagrams. The positions of the Flinn diagrams approximately correspond to those of the block diagrams below. Also shown is the direction of the instantaneous stretching axes and fields of instantaneous contraction (black) and extension for dextral simple shear.

differently than the surrounding medium to the overall deformation, and such markers are called **active markers**.

An example of data from active strain markers is shown in Figure 3.11. These data were collected from a deformed polymictic conglomerate where three-dimensional strain has been estimated from different clast types in the same rock and at the same locality. Clearly, the different clast types have recorded different amounts of strain. Competent (stiff) granitic clasts are less strained than less competent greenstone clasts. This is seen using the fact that strain intensity generally increases with increasing distance from the origin in Flinn space. But there is another interesting thing to note from this figure: It seems that competent clasts plot higher in the Flinn diagram (Figure. 3.11) than incompetent ("soft") clasts, meaning that competent clasts take on a more prolate shape. Hence, not only strain intensity but also strain geometry may vary according to the mechanical properties of strain markers.

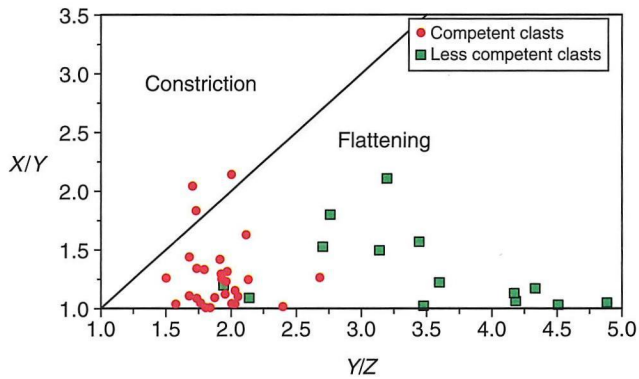

Figure 3.11 Strain obtained from deformed conglomerates, plotted in the Flinn diagram. Different pebble types show different shapes and finite strains. Polymict conglomerate of the Utslettefjell Formation, Stord, southwest Norway. Data collected by D. Kirschner, R. Malt and the author.

The way that the different markers behave depends on factors such as their mineralogy, preexisting fabric, grain size, water content and temperature–pressure conditions at the time of deformation. In the case of Figure 3.11, the temperature–pressure regime is that of lower to middle greenschist facies. At higher temperatures, quartz-rich rocks are more likely to behave as "soft" objects, and the relative positions of clast types in Flinn space are expected to change.

The last point above also requires attention: the initial shape of a deformed object clearly influences its post-deformational shape. If we consider two-dimensional objects such as sections through oolitic rocks, sandstones or conglomerates, the R_f/ϕ method discussed above can handle this type of uncertainty. It is better to measure up two or more sections through a deformed rock using this method than dig out an object and measure its three-dimensional shape. The single object could have an unexpected initial shape (conglomerate clasts are seldom perfectly spherical or elliptical), but by combining numerous measurements in several sections we get a statistical variation that can solve or reduce this problem.

Three-dimensional strain is usually found by combining two-dimensional data from several differently oriented sections.

There are now computer programs that can be used to extract three-dimensional strain from sectional data. If the sections each contain two of the principal strain axes everything becomes easy, and only two are strictly needed (although three would still be good). Otherwise, strain data from at least three sections are required.

Summary

Strain markers in deformed rocks reveal how much the rock has been strained, and information about the nature of the deformation (e.g. flattening versus constriction, and the direction of strain axes) can be obtained. This is very useful when trying to understand what has happened to a deformed region, and when searching for a model for the deformation. The way that rocks accumulate strain depends on the stress field, boundary conditions, physical properties of the rock as well as external factors such as temperature, pressure and state of stress. In the next few chapters we will explore some of these relationships. Some key points to review and questions to address:

- Strain is only revealed by means of new deformation structures (cleavage, shear zones, fractures) or by means of preexisting markers that have changed shape during deformation.
- Strain analysis requires knowledge about the shape or geometry of strain markers before the deformation initiated.
- Objects that were circular or spherical before deformation are ideal, but non-spherical objects with a spread in initial orientations can also be used.

- Several techniques and computer codes exist that can help us extract strain from deformed rocks.
- Always look for objects, layers or linear features that can reveal strain in deformed rocks.

Review questions

1. What is meant by the term "strain marker"? Give examples.
2. What information can we obtain from linear or planar strain markers?
3. What is the effect of a viscosity (competence) difference between strain markers and the matrix?
4. How can we deal with pre-deformational fabrics, for example in conglomerate pebbles?
5. What is needed to find shear strain in a rock?
6. Give some serious concerns (pitfalls) regarding strain analysis.
7. How much shear strain has the trilobite in Figure 3.3 experienced parallel to its axial line?
8. How can we find three-dimensional strain from a deformed conglomerate?
9. Shear zones are expressions of heterogeneous strain. How can we perform strain analyses in shear zones?
10. What is meant by strain partitioning in this context?

E-MODULE

The e-module *Strain* is recommended for this chapter.

FURTHER READING

Numerical calculations

Mookerjee, M., and Nickleach, S., 2011, Three-dimensional strain analysis using Mathematica. *Journal of Structural Geology* **33**: 1467–1476.

Mulchrone, K. F., and Chowdhury, K. R., 2004, Fitting an ellipse to an arbitrary shape: implications for strain analysis. *Journal of Structural Geology* **26**: 143–153.

Shan, Y., 2008, An analytical approach for determining strain ellipsoids from measurements on planar surfaces. *Journal of Structural Geology* **30**: 539–546.

Shimamoto, T., Ikeda, Y., 1976, A simple algebraic method for strain estimation from ellipsoidal objects. *Tectonophysics* **36**: 315–337.

Strain associated with cleavage

Goldstein, A., Knight, J. and Kimball, K., 1999, Deformed graptolites, finite strain and volume loss during cleavage formation in rocks of the taconic slate belt, New York and Vermont, U.S.A. *Journal of Structural Geology* **20**: 1769–1782.

Strain ellipsoid from sectional data

De Paor, D. G., 1990, Determination of the strain ellipsoid from sectional data. *Journal of Structural Geology* **12**: 131–137.

Strain techniques in more detail

Erslev, E. A., 1988. Normalized center-to-center strain analysis of packed aggregates. *Journal of Structural Geology* **10**: 201–209.

Lisle, R., 1985, *Geological Strain Analysis*. Amsterdam: Elsevier.

Ramsay, J. G. and Huber, M. I., 1983, *The Techniques of Modern Structural Geology. Vol. 1: Strain Analysis*. London: Academic Press.

Three-dimensional strain

Bhattacharyya, P. and Hudleston, P., 2001, Strain in ductile shear zones in the Caledonides of northern Sweden: a three-dimensional puzzle. *Journal of Structural Geology* **23**: 1549–1565.

Holst, T. B. and Fossen, H., 1987, Strain distribution in a fold in the West Norwegian Caledonides. *Journal of Structural Geology* **9**: 915–924.

Hossack, J., 1968, Pebble deformation and thrusting in the Bygdin area (Southern Norway). *Tectonophysics* **5**: 315–339.

Strine, M. and Wojtal, S. F., 2004, Evidence for non-plane strain flattening along the Moine thrust, Loch Srath nan Aisinnin, North-West Scotland. *Journal of Structural Geology* **26**, 1755–1772.